A&A 644, A147 (2020)
https://doi.org/10.1051/0004-6361/202037654

Astronomy & Astrophysics

Constraints on the astrophysical environment of binaries with gravitational-wave observations

Vitor Cardoso[1] and Andrea Maselli[2]

[1] CENTRA, Departamento de Física, Instituto Superior Técnico – IST, Universidade de Lisboa – UL, Avenida Rovisco Pais 1, 1049 Lisboa, Portugal
e-mail: vitor.cardoso@tecnico.ulisboa.pt
[2] Dipartimento di Fisica, "Sapienza" Università di Roma & Sezione INFN Roma1, P. A. Moro 5, 00185 Roma, Italy
e-mail: andrea.maselli@roma1.infn.it

Received 4 February 2020 / Accepted 9 November 2020

ABSTRACT

Aims. The dynamics of coalescing compact binaries can be affected by the environment in which the systems evolve, leaving detectable signatures in the emitted gravitational signal. In this paper, we investigate the ability of gravitational-wave detectors to constrain the nature of the environment in which compact binaries merge.
Methods. We parametrized a variety of environmental effects by modifying the phase of the gravitational signal emitted by black hole and neutron star binaries. We infer the bounds on such effects by current and future generations of interferometers, studying their dependence on the binary's parameters.
Results. We show that the strong dephasing induced by accretion and dynamical friction can constrain the density of the surrounding medium to orders of magnitude below those of accretion disks. Planned detectors, such as LISA or DECIGO, will be able to probe densities typical of those of dark matter.

Key words. gravitational waves – black hole physics

1. Introduction

Most of the content of our Universe is unknown, and its properties may change from the solar neighborhood to distant galaxies. Accordingly, the astrophysical environment around stellar and massive black holes (BHs) can be very diverse. The dark matter density in the solar neighborhood is of order $\rho = 0.01 M_\odot\,\mathrm{pc}^{-3} = 6.7\times10^{-22}\,\mathrm{kg\,m}^{-3}$ (Pato et al. 2015), and that of interstellar dust can be even lower. However, the dark matter density can be eight orders of magnitude (or more) larger, close to the center of galaxies and in the vicinities of BHs (Ferrer et al. 2017). Supermassive BH binaries can evolve in accretion disks, which have baryonic densities as large as 10^{-6}–$100\,\mathrm{kg\,m}^{-3}$ for thick and thin accretion disks, respectively (Barausse et al. 2014). It has also been conjectured that coalescing BHs may form via dynamical fragmentation of a very massive star undergoing gravitational collapse, leading to a binary evolving in a medium with density as high as $10^{10}\,\mathrm{kg\,m}^{-3}$ or higher (Loeb 2016; Reisswig et al. 2013)[1].

In the presence of a nontrivial environment (magnetic fields, fluids, dark matter, etc.), three mechanisms contribute to changing the dynamics of a compact binary with respect to that in a vacuum: accretion, gravitational drag, and the self-gravity of the fluid. These all contribute to a small, but potentially observable change of the gravitational-wave (GW) phase. We wish to understand on which level GW observations can constrain the properties of the environment, with only mild assumptions.

[1] However, the lack of any counterparts for the LIGO-Virgo binary BH sources is evidence that such extreme scenarios are not common.

2. The phase dependence in the vacuum and beyond

2.1. Setup

Take a BH binary of total mass $M = m_1 + m_2$, with $m_{1,2}$ component masses separated by a distance L and with an orbital frequency Ω. Although the orbit is generically eccentric, GW emission tends to circularize it on relatively short timescales (Peters 1964; Krolak & Schutz 1987). This is certainly true for stellar mass BH binaries, which form substantially prior to merger and evolve mostly only via GW emission. However, the formation of supermassive BH binaries is poorly understood. Some of the mechanisms that contribute to the forming and merging of such binaries may actually also impart a substantial eccentricity, specially in its initial stages (Barack et al. 2019). However, even in such a scenario the evolution of such systems quickly reduces eccentricity (Shapiro Key & Cornish 2011). Here, we always assume that the binary has circularized by the time it enters the detector band. At leading order in vacuum GR, binary dynamics are governed by energy balance: the quadrupole formula implies that the binary is emitting a flux of GW energy:

$$\dot{E}_{\rm GW} = \frac{32}{5}\mu^2 L^4 \Omega^6\,, \tag{1}$$

in GWs, where $\mu = m_1 m_2/M$ is the reduced mass of the system. Thus, the orbital energy of the system $E_{\rm orb} = -M\mu/(2L)$ must decrease at a rate fixed by such loss. This immediately fixes the time dependence of the GW frequency to $f^{-8/3} = (8\pi)^{8/3}\mathcal{M}^{5/3}(t_0 - t)/5$, where $\mathcal{M} = M\eta^{3/5}$ is the chirp mass, $\eta = m_1 m_2/M^2 = \mu/M$ the symmetric mass ratio, and $f = \Omega/\pi$.

Once the frequency evolution is known, the GW phase simply reads

$$\varphi(t) = 2\int^{t} \Omega(t')\mathrm{d}t' \,. \tag{2}$$

In Fourier domain, it is possible to obtain analytical templates of the waveforms. One can write the metric fluctuations as

$$h_+(t) \;=\; A_+(t_{\rm ret})\cos\varphi(t_{\rm ret})\,, \tag{3}$$
$$h_\times(t) \;=\; A_\times(t_{\rm ret})\sin\varphi(t_{\rm ret})\,, \tag{4}$$

where $t_{\rm ret}$ is the retarded time. The Fourier-transformed quantities are

$$\tilde{h}_+ = \mathcal{A}_+ e^{i\Psi_+}\,, \qquad \tilde{h}_\times = \mathcal{A}_\times\, e^{i\Psi_\times}\,. \tag{5}$$

Dissipative effects are included within the stationary phase approximation, where the secular time evolution is governed by the GW emission (Flanagan & Hughes 1998). In Fourier space, we decompose the phase of the GW signal $\tilde{h}(f) = \mathcal{A}e^{i\Psi(f)}$ as follows:

$$\Psi(f) = \Psi^{(0)}_{\rm GR}[1 + (\text{PN corrections}) + \delta_{\Psi_{\rm env}}]\,, \tag{6}$$

where $\Psi^{(0)}_{\rm GR} = 3/128(\mathcal{M}\pi f)^{-5/3}$ represents the leading term of the phase's post-Newtonian (PN) expansion.

2.2. Corrections to the GW phase due to environmental effects

Environmental effects on the evolution of a compact binary can be divided into different categories, and they have been comprehensibly studied in the past (Yunes et al. 2011; Kocsis et al. 2011; Eda et al. 2013; Macedo et al. 2013; Barausse et al. 2014). We summarize here the results of Barausse et al. (2014) extending them to generic density profiles. We consider a BH binary evolving in a medium of density:

$$\rho = \rho_0 (R/r)^\beta \,. \tag{7}$$

This density profile can describe a constant magnetic field or constant-density fluid for $\beta = 0$, or thick accretion disks. Studies of fuzzy dark matter, described by ultralight scalars, show that close to the galactic centers the density is approximately constant, $\beta \approx 0$ (Hui et al. 2017; Annulli et al. 2020). On the other hand, particle-like dark matter (with small Compton wavelength) is described by $\beta = 1$ in the inner core of dark matter regions (Navarro et al. 1997; Gondolo & Silk 1999; Sadeghian et al. 2013). However, such large overdensities are easily washed out via scattering of stars or BHs, or accretion by the central BH, induced by heating in its vicinities (Merritt et al. 2002; Bertone & Merritt 2005; Merritt 2004). These effects tend to smooth the dark matter density close to the galaxy centers. We thus take $\beta = 0$ to describe most of the known environment around compact binaries well. We note that an arbitrary density profile is locally constant, and therefore $\beta \approx 0$ for the physics of compact binaries, the focus of this work.

Such an environment affects binary dynamics in different ways: by exerting a gravitational pull on the binary, the Newtonian equation of motion and balance equations change, leading to a relative dephasing:

$$\delta^{\rm grav\ pull}_{\Psi_{\rm env}} \approx \rho_0 f^{\frac{2\beta}{3}-2} M^{-\beta/3} R^\beta \,, \tag{8}$$

up to factors of order unity, which is in agreement with previous results (Eda et al. 2013; Barausse et al. 2014).

Accretion of the surrounding medium into the BH also introduces a dephasing. This can be estimated by assuming a fluid at rest (with no angular momentum) and unperturbed by the binary. The dephasing introduced by accretion can be computed by extending previous analysis (Macedo et al. 2013; Barausse et al. 2014). The result depends on the type of accretion (i.e., if the environmental medium is collisionless or behaves as a fluid). We find

$$\delta^{\rm accretion}_{\Psi_{\rm env}} \approx \begin{cases} -\dfrac{R^\beta\rho_0}{\eta^{2/5}\mathcal{M}^{1+\frac{\beta}{3}}}(\pi f)^{\frac{2\beta}{3}-3} & \text{collisionless} \\ -\dfrac{(1-3\eta)R^\beta\rho_0}{\eta^2\mathcal{M}^{\frac{5}{3}+\frac{\beta}{3}}}(\pi f)^{\frac{2\beta}{3}-\frac{11}{3}} & \text{Bondi} \end{cases} . \tag{9}$$

Besides the extra gravitational pull by the matter inside the orbital radius and accretion, all of the surrounding medium slows the binary down through gravitational drag. At leading order, the gravitational drag produces a force on object "i" in the direction of motion, given by

$$F_{\rm DF} = \frac{4\pi\rho(GM_i)^2}{v_i^2} I, \tag{10}$$

where v is the relative velocity between body "i" and the gas (which we take, as a rough approximation, to be given by the Keplerian velocity), and I is a prefactor of order unity that depends on the relative velocity of the binary components with respect to the medium (Kim & Kim 2007).

For supersonic motion, $I \sim \ln[(r_i/r_{\rm min})/(0.11\Upsilon + 1.65)]$, with $\Upsilon \equiv v/v_{\rm s}$ the Mach number ($v_{\rm s}$ is the sound speed), r_i the orbital radius of the object, and $r_{\rm min}$ an unknown fitting parameter. Our results show a very mild dependence on the exact value of $r_{\rm min}$. There are special-relativistic corrections to this formula (Barausse 2007), and corrections for slab-like geometries (such as those in accretion disks) (Vicente et al. 2019). We do not consider these effects here. Relativistic effects are expected to have a negligible impact: dynamical friction on a straight-moving object is affected by a correction term of the order $(1+v^2)^2\Gamma^2$, with Γ the Lorentz factor and v the relative velocity (Barausse 2007). Even for $v = 0.1$, this introduces a correction of only 22% in the dynamical friction, which does not affect our order-of-magnitude estimates. The geometry of the environment, on the other hand, may be relevant for thin accretion disks. When the motion is supersonic, geometry may suppress friction by a factor two (Vicente et al. 2019). Suppression is stronger for subsonic motion.

The dephasing introduced by dynamical friction is regulated by an extra energy loss $\dot{E}_{\rm DF} = F_{\rm DF} v_K$. For the profile (7), we find the dephasing,

$$\delta^{\rm DF}_{\Psi_{\rm env}} \approx -\frac{(1-3\eta)R^\beta\rho_0}{\eta^2\mathcal{M}^{\frac{1}{3}(\beta+5)}}(\pi f)^{\frac{2\beta}{3}-\frac{11}{3}} \,. \tag{11}$$

The results for the dephasing can all be captured by the expression

$$\delta_{\Psi_{\rm env}} = \kappa_\beta M^{2-\beta} R^\beta \rho_0 (Mf)^{-\gamma} \,, \tag{12}$$

up to factors of order unit, where the exponent γ and the precise coefficient κ_β are listed in Table 1. The parameter β only affects the results via a simple re-scaling of the $\beta = 0$ results. In the rest of this work we focus on $\beta = 0$: in this case the most constraining

Table 1. Corrections $\delta_{\Psi_{\rm env}} = \kappa_\beta \rho_0 M^{2-\beta} R^\beta (Mf)^{-\gamma}$ to the GW phase in the Fourier space computed within the stationary phase approximation for a quasi-circular binary (see Eq. (12)).

Mechanism	$\gamma_{(\beta=0)}$	κ_0	$\gamma_{(\beta=1)}$	κ_1
Gravitational pull	2	1	4/3	1
Gravitational drag	11/3	$-\eta^{-3}(1-3\eta)\pi^{-11/3}$	3	$-\eta^{-16/5}(1-3\eta)\pi^{-3}$
Accretion – Bondi	11/3	$-\eta^{-3}(1-3\eta)\pi^{-11/3}$	3	$-\eta^{-16/5}(1-3\eta)\pi^{-3}$
Accretion – collisionless	3	$-\eta^{-1}\pi^{-3}$	7/3	$-\eta^{-6/5}\pi^{-7/3}$

Notes. The binary moves in a medium of density $\rho = \rho_0 (R/r)^\beta$, and it is subjected to accretion, gravitational forces from the matter distribution (assumed to be centered at the binary's center of mass), and to gravitational drag. Results refer to $\beta = (0, 1)$ and to collisionless and Bondi accretion, respectively.

effect is given by the gravitational drag, and it is controlled by $\gamma = 11/3$.

Finally, we note that the corrections introduced by environmental effects modify the phasing at very low (and negative) pre-Newtonian order. They can all be included in a parametrized formalism (Yunes & Pretorius 2009a; Barausse et al. 2014; Abbott et al. 2016). Some of these modifications of the PN series were already considered in the context of extra radiation channels, with an unknown underlying physical theory (Barausse et al. 2016; Carson et al. 2020; Gnocchi et al. 2019). The results above show that such modifications appear at $n = -3\gamma/2$ PN order, and have a very specific physical origin.

Our intention now is to constrain, at an order-of-magnitude level and agnostically, the environmental properties. Although the drag created by thin accretion disks falls outside the approximations made here for the density, it can be mapped into one of the above with $\beta = 15/8$ (Barausse et al. 2014).

2.3. Measurement uncertainties: a fisher matrix analysis

A comprehensive survey of the impact of several environmental effects in the GW signal is shown in Barausse et al. (2014) through an estimate of the signal dephasing with respect to that of vacuum GR. Here, we wish to quantify the precision with which current and planned detectors are able to constrain environmental properties. As a baseline for the GR waveform, we used the semi-analytical PhenomB[2] template in the frequency domain for non-precessing spinning BHs (Ajith et al. 2008, 2011). We considered a Newtonian amplitude, averaging on the sky localization of the binary systems. In the limit of GW signals with large signal-to-noise ratios (S/Ns), the probability distribution of the source's parameters, for a given observation, can be described by a multivariate Gaussian peaked around the true values, and with covariance $\Sigma_{ij} = (\Gamma^{-1})_{ij}$, given by the inverse of the Fisher matrix (Vallisneri 2008). The latter is built from the first derivatives of the GW template $\tilde{h}(f) = \mathcal{A} \exp[i(\Psi_{\rm GR} + \psi_{\rm env})]$ with respect to the source's parameters $\theta_i = (\ln \mathcal{M}, \ln \eta, \tau_c, \phi_c, \chi_{\rm eff}, \rho_0)$:

$$\Gamma_{ij} = \int_{f_{\rm min}}^{f_{\rm max}} \frac{1}{S_{\rm n}(f)} \frac{\partial \tilde{h}}{\partial \theta_i} \frac{\partial \tilde{h}}{\partial \theta_j} {\rm d}f. \tag{13}$$

The uncertainties on θ_i are given by the diagonal components of the covariance matrix, namely $\sigma_i = \sqrt{\Sigma_{ii}}$. Beside the chirp mass, the GW template depends on the symmetric mass ratio η, on the time and phase at the coalescence (τ_c, ϕ_c), and on the effective spin $\chi_{\rm eff} = (m_1\chi_1 + m_2\chi_2)/M$, where $\chi_{1,2}$ are the BH's dimensionless spin parameters. The integral in Eq. (13) is also a function of the detector's noise spectral density $S_{\rm n}(f)$. In our analysis, we focus on both ground- and space-based interferometers. We consider advanced LIGO/Virgo at design sensitivity (LIGOWhite 2018), a third-generation detector such as the *Einstein* Telescope (Hild et al. 2011; ETWhite 2018; see also Abbott et al. 2017 for other proposals of third-generation ground-based detectors like the Cosmic Explorer), the LISA mission (Amaro-Seoane et al. 2017), and the Japanese satellite DECIGO, proposed to operate in the decihertz regime (Isoyama et al. 2018). The lower end of the Fisher matrix's integration is set to $f_{\rm min}^{\rm LIGO/Virgo} = 10$ Hz, $f_{\rm min}^{\rm ET} = 3$ Hz and $f_{\rm min}^{\rm DECIGO} = 0.01$ Hz. For LISA, we chose $f_{\rm min}^{\rm LISA}$ as the frequency value of the binary four years before the merger (Berti et al. 2005). On the other edge of the integral, we set the maximum frequency of ground based detectors to coincide with the PhenomB inspiral-merger transition value $f_{\rm 1M}$, which depends on the source's parameters (Ajith et al. 2011), while for space interferometers, $f_{\rm max}^{\rm LISA} = \min[1\ {\rm Hz}, f_{\rm 1M}]$ and $f_{\rm max}^{\rm DECIGO} = \min[100\ {\rm Hz}, f_{\rm 1M}]$. Given the frequency content of the astrophysical corrections (8)–(9) and (11), we expect $f_{\rm max}$ to have a small effect on the uncertainties inferred through the Fisher matrix (Barausse et al. 2014).

3. Results: the ability of GW detectors to constrain environmental densities

As prototype binaries for our numerical analysis, we considered five classes of objects: (i) two stellar mass BH binary systems with the properties of the observed gravitational events GW150915 and GW170608, and the binary neutron star event GW170817 (Abbott et al. 2018); (ii) a massive binary (MBBH) with $(m_1, m_2) = (10^6, 5\times10^5) M_\odot$ and $(\chi_1, \chi_2) = (0.9, 0.8)$; (iii) an intermediate-mass binary (IBBH) with $(m_1, m_2) = (10^4, 5\times10^3) M_\odot$ and $(\chi_1, \chi_2) = (0.3, 0.4)$; (iv) an intermediate mass ratio inspiral (IMRI), where $(m_1, m_2) = (10^4, 10) M_\odot$ and $(\chi_1, \chi_2) = (0.8, 0.5)$; (v) and finally an extreme mass ratio binary (EMRI) with $(m_1, m_2) = (10^5, 10) M_\odot$ and spin parameters $(\chi_1, \chi_2) = (0.8, 0.5)$.

All massive sources targeted by LISA are located at 1 Gpc from the detector, while for the stellar binaries we used the median values of the luminosity distance estimated by the LIGO/Virgo collaboration. Depending on the interferometer and on the luminosity distance, the binaries feature different S/Ns. For MBBH, IBBH, EMRIs, and IMRIs detected by LISA, the S/N is $\simeq 3\times10^4$, $\simeq 708$, $\simeq 22$, and $\simeq 64$, respectively. For the stellar mass systems in (i), (a) $({\rm SNR}^{\rm Dec}, {\rm SNR}^{\rm ET}, {\rm SNR}^{\rm LIGO}) \simeq (2815, 615, 40)$ for GW150914; (b) $({\rm SNR}^{\rm Dec}, {\rm SNR}^{\rm ET}, {\rm SNR}^{\rm LIGO}) \simeq$

[2] The waveform corrections described in the previous section belong to the class of "pre-Newtonian" modifications, and they affect the signal at very low frequencies, where PhenomB is indistinguishable from more sophisticated templates (Yunes & Pretorius 2009b).

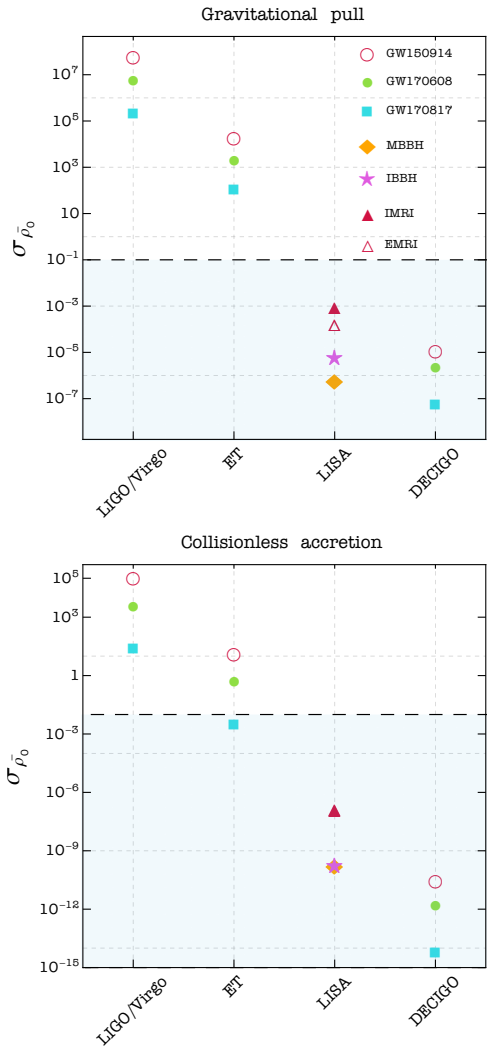

Fig. 1. 1-σ uncertainties on density parameter ρ_0 normalized to the average density of water $\rho_{H_2O} \simeq 10^3 \mathrm{kg\,m^{-3}}$ for different sources and detector configurations. *Top and bottom panels*: environmental effects due to gravitational pull and collisionless accretion. Different point markers identify distinct sources. For ground-based detectors and for DECIGO, we considered sources with the same parameters of GW150914, GW170608, and GW170817 (Abbott et al. 2018). For LISA, we considered a massive and intermediate-massive systems, as well as IMRI and EMRI, all located at $d = 1$ Gpc from the detector. The gray area denotes densities typical of accretion disks.

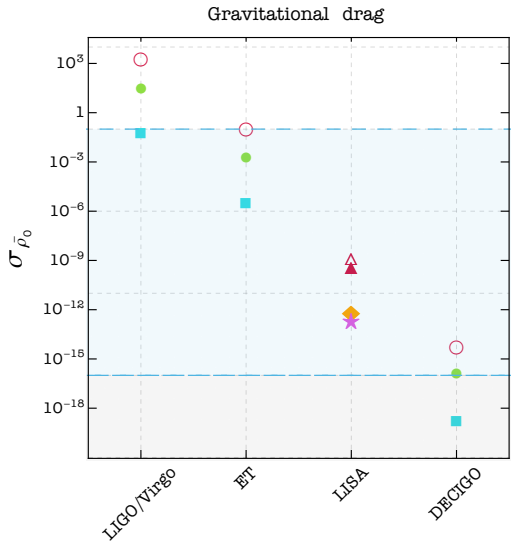

Fig. 2. 1-σ uncertainties on density parameter ρ_0 normalized to the water average density for sources and detector configurations already shown in Fig. 1, obtained via (a lack of) dephasing from dynamical friction. The shaded blue area denotes densities typical or smaller than those of accretion disks, while the gray shaded region denotes densities typical of dark matter.

(1290, 303, 21) for GW170608; and (c) $(\mathrm{SNR}^{\mathrm{Dec}}, \mathrm{SNR}^{\mathrm{ET}}, \mathrm{SNR}^{\mathrm{LIGO}}) \simeq (2124, 502, 35)$ for GW170817.

We used the Fisher matrix analysis above to study the lowest environmental densities that different GW detectors are able to constrain. To be more specific, we studied the critical density ρ_0 for which $\sigma_{\rho_0} \lesssim \rho_0$, the threshold for densities below which observations are unable to distinguish between vacuum and a nontrivial environmental density. Numerical values of the 1-σ uncertainties on the parameter ρ_0 are shown in Figs. 1 and 2 for the three environmental effects discussed in the previous section. We opted to normalize these results by the average density of the water $\rho_{H_2O} \simeq 10^3 \mathrm{kg\,m^{-3}}$, defining $\bar{\rho}_0 = \rho/\rho_{H_2O}$. This is an ad-hoc choice made only for visual clarity of the figures.

Figure 1 shows that the gravitational pull of matter, even when optimized (we centered the environment at the binary's center of mass to maximize the effects of the pull) can provide only weak constraints. For a double neutron star, LIGO is able to bound the surrounding density to level 100 000 smaller than that of water. The blue-shaded area in all figures indicates ranges of density of the order of those of accretion disks. As we can see, even using only the gravitational pull or accretion effects, future detectors will probe this region. Accretion effects are more important, and the *Einstein* Telescope can already probe environmental densities that can be of order of those expected for thin accretion disks.

As expected from the correspondence between the exponent γ and the post-Newtonian order, the most constraining effect is that of gravitational drag, which appears at -5.5 PN order. Although the data shown in Figs. 1 and 2 correspond to a specific binary location, our results can immediately be rescaled to any value of the source's luminosity distance, as the uncertainties are proportional to the inverse of d.

For stellar-mass binaries, the tightest constraints on the density ρ_0 are provided by DECIGO, yielding bounds several orders of magnitude stronger than those obtained with current and future generation of ground-based detectors. Constraints inferred by the Japanese satellite are also tighter than those derived from the observation of intermediate and massive sources in the millihertz regime by LISA. The best-case scenario is given by the double neutron star system, GW170817, and in general by very light sources. The latter span a large number of cycles in the low-frequency part of the spectrum, in which environmental effects are more important.

Results for the gravitational drag are particularly interesting. Advanced detectors may be able to constrain the parameter ρ_0 at values close to the typical densities of thin accretion disks. A third generation of detectors supplied by low-mass observations would also be able to probe densities featured by thick accretion disks. These values improve dramatically for space interferometers. Numerical data for DECIGO show that neutron star binaries are in principle able to constrain the lack of dephasing from dynamical friction at the level of dark matter density, namely for $\rho \ll 10^{-18} \mathrm{kg\,m^{-3}}$. Such results also extend

to the case of Bondi accretion, for which the phase correction $\delta\Psi_{\rm env}$ is characterized by the same exponent γ, and therefore by the same -5.5 PN order.

4. Conclusions

Gravitational wave observations of compact binary coalescences represent an established field of research, which maps the high-energy Universe detecting sources at various distances and orientations in the sky. Advanced detectors like LIGO/Virgo are now close to reaching their full sensitivity, and will be soon joined by the Japanese KAGRA (Akutsu et al. 2019). Moroever, third-generation ground-based detectors, as well as future space-based facilities, will make GW detections a weekly routine. The quantity and the quality of this incoming flood of data will make it possible to deepen our understanding of compact objects (Barack et al. 2019; Cardoso & Pani 2019), and at the same time to investigate the arena in which they evolve.

This work represents a step forward in this direction, showing how GW detectors have a tremendous potential to constrain the properties of different phenomena occurring during the coalescence of binary sources. We focused on three main effects: the gravitational drag, collisionless accretion, and the gravitational pull, showing how observations translate into precise bounds on the binary environmental density. We investigated the precision of future measurements of this parameter by suitable modifications of the signal emitted by different families of compact objects. Our results are agnostic as to the nature of the environment, but can be easily mapped to specific models. The bound inferred by space detectors such as LISA and DECIGO are so tight that one can consider using GW detectors to exclude large dark matter overdensities close to the binary location.

The description given in this paper of dynamical friction holds for fluid-like environments, composed of particles with a small Compton wavelength. The calculation of dynamical friction for ultralight fields with a Compton wavelength, which is large when compared to the binary parameters, was completed after the completion of Annulli et al. (2020). This analysis predicts a dephasing $\delta\Psi_{\rm env}$ described by Eq. (12) with $\gamma = 4$. We repeated the analysis described in the main text for such a value of γ, finding that the detection of an IBBH with LISA will improve constraints on the density by more than an order of magnitude.

Our results assume that systematics – such as uncertainties in computing the vacuum waveforms – are under control. In this context, we tested our calculations by varying the template used for the Fisher analysis. This was done by (i) neglecting, for example, the contribution of the late inspiral/merger phase, and (ii) adding new parameters that can model missing physical effects, like tidal interactions. The uncertainties on the environmental parameters are robust against these changes, with relative differences of the order of sub-percent. The only exception is given by EMRIs/IMRIs, where for case (i) we find larger deviations on $\sigma_{\tilde{\rho}_0}$, still $\lesssim 40\%$. Overall, these changes do not alter the conclusions of our analysis. Our results are, naturally, a source of degeneracy and a limiting factor for tests of gravity (Barausse et al. 2014; Yunes et al. 2016): some of these astrophysical effects might be dominant over possible modifications of general relativity. The estimates of the leading post-Newtonian effects on the waveforms are simplistic, done in a Newtonian setup, and neglect a back-reaction on the medium itself. For equal-mass mergers, this may mean that our drag estimates overestimate the actual effect. Dynamical friction was treated at the nonrelativistic level and neglecting effects of the geometry of the environment. Such effects may be important for thin accretion disks, for example, but the generalization of the results of Vicente et al. (2019) regarding circular motion is still missing. Possible multiband detections were not explored here, but they will improve the bound we discussed even further. Our results highlight the amazing possibilities of GW astronomy, but also highlight the need to understand, in detail, the evolution of massive binaries within nontrivial environments.

Acknowledgements. V.C. acknowledges financial support provided under the European Union's H2020 ERC Consolidator Grant "Matter and strong-field gravity: New frontiers in Einstein's theory" grant agreement no. MaGRaTh–646597. A.M acknowledges support from the Amaldi Research Center funded by the MIUR program "Dipartimento di Eccellenza" (CUP: B81I18001170001). This project has received funding from the European Union's Horizon 2020 research and innovation programme under the Marie Sklodowska-Curie grant agreement No 690904. We acknowledge financial support provided by FCT/Portugal through grant PTDC/MAT-APL/30043/2017. The authors would like to acknowledge networking support by the GWverse COST Action CA16104, "Black holes, gravitational waves and fundamental physics."

References

Abbott, B. P., Abbott, R., Abbott, T. D., et al. 2016, Phys. Rev. Lett., 116, 221101; Erratum: Phys. Rev. Lett., (2018) 121, 129902
Abbott, B. P., Abbott, R., Abbott, T. D., et al. 2017, Class. Quant. Grav., 34, 044001
Abbott, B. P., Abbott, R., Abbott, T. D., et al. 2018, Phys. Rev. X, 9, 031040
Ajith, P., Babak, S., Chen, Y., et al. 2008, Phys. Rev. D, 77, 104017; Erratum: Phys. Rev., D (2009) 79, 129901
Ajith, P., Hannam, M., Husa, S., et al. 2011, Phys. Rev. Lett., 106, 241101
Akutsu, T., Ando, M., Arai, K., et al. 2019, Nat. Astron., 3, 35
Amaro-Seoane, P., Audley, H., Babak, S., et al. 2017, ArXiv e-prints [arXiv:1702.00786]
Annulli, L., Cardoso, V., & Vicente, R. 2020, Phys. Lett. B, 811, 135944
Barack, L., Cardoso, V., Nissanke, S., et al. 2019, Class. Quant. Grav., 36, 143001
Barausse, E. 2007, MNRAS, 382, 826
Barausse, E., Cardoso, V., & Pani, P. 2014, Phys. Rev., D89, 104059
Barausse, E., Yunes, N., & Chamberlain, K. 2016, Phys. Rev. Lett., 116, 241104
Berti, E., Buonanno, A., & Will, C. M. 2005, Phys. Rev. D, 71, 084025
Bertone, G., & Merritt, D. 2005, Phys. Rev. D, 72, 103502
Cardoso, V., & Pani, P. 2019, Liv. Rev. Rel., 22, 4
Carson, Z., Seymour, B. C., & Yagi, K. 2020, Classical and Quantum Gravity, 37, 065008
Eda, K., Itoh, Y., Kuroyanagi, S., & Silk, J. 2013, Phys. Rev. Lett., 110, 221101
ETWhite 2018, https://tds.virgo-gw.eu/?content=3&r=14065
Ferrer, F., da Rosa, A. M., & Will, C. M. 2017, Phys. Rev. D, 96, 083014
Flanagan, E. E., & Hughes, S. A. 1998, Phys. Rev. D, 57, 4535
Gnocchi, G., Maselli, A., Abdelsalhin, T., Giacobbo, N., & Mapelli, M. 2019, Phy. Rev. D, 100, 064024
Gondolo, P., & Silk, J. 1999, Phys. Rev. Lett., 83, 1719
Hild, S., Abernathy, M., Acernese, F., et al. 2011, Class. Quant. Grav., 28, 094013
Hui, L., Ostriker, J. P., Tremaine, S., & Witten, E. 2017, Phys. Rev. D, 95, 043541
Isoyama, S., Nakano, H., & Nakamura, T. 2018, PTEP, 2018, 073E01
Kim, H., & Kim, W.-T. 2007, ApJ, 665, 432
Kocsis, B., Yunes, N., & Loeb, A. 2011, Phys. Rev. D, 84, 024032
Krolak, A., & Schutz, B. F. 1987, Gen. Rel. Grav., 19, 1163
LIGOWhite 2018, https://dcc.ligo.org/LIGO-T1800044/public
Loeb, A. 2016, ApJ, 819, L21
Macedo, C. F., Pani, P., Cardoso, V., & Crispino, L. C. 2013, ApJ, 774, 48
Merritt, D. 2004, Phys. Rev. Lett., 92, 201304
Merritt, D., Milosavljevic, M., Verde, L., & Jimenez, R. 2002, Phys. Rev. Lett., 88, 191301
Navarro, J. F., Frenk, C. S., & White, S. D. M. 1997, ApJ, 490, 493
Pato, M., Iocco, F., & Bertone, G. 2015, JCAP, 1512, 001
Peters, P. 1964, Phys. Rev., 136, B1224
Reisswig, C., Ott, C. D., Abdikamalov, E., et al. 2013, Phys. Rev. Lett., 111, 151101
Sadeghian, L., Ferrer, F., & Will, C. M. 2013, Phys. Rev. D, 88, 063522
Shapiro Key, J., & Cornish, N. J. 2011, Phys. Rev. D, 83, 083001
Vallisneri, M. 2008, Phys. Rev. D, 77, 042001
Vicente, R., Cardoso, V., & Zilhão, M. 2019, MNRAS, 489, 5424
Yunes, N., & Pretorius, F. 2009a, Phys. Rev. D, 80, 122003
Yunes, N., & Pretorius, F. 2009b, Phys. Rev. D, 79, 084043
Yunes, N., Kocsis, B., Loeb, A., & Haiman, Z. 2011, Phys. Rev. Lett., 107, 171103
Yunes, N., Yagi, K., & Pretorius, F. 2016, Phys. Rev. D, 94, 084002